FINAL REPORT ON INTERCALIBRATION AND CROSS-CORRELATION OF ACE AND WIND SOLAR WIND DATA

NASA GRANT NUMBER: NAG5-7794
MIT OSP NUMBER: 6792900

1. INTRODUCTION

This report covers activities funded from October 1, 1998 through September 30, 2002. Two yearly status reports have been filed on this grant, and they are included as Appendix 1.

The purpose of this grant was to compare *ACE* and *Wind* solar wind parameters when the two spacecraft were near to one another and then to use the intercalibrated parameters to carry out scientific investigations. In September, 2001 a request for a one-year, no-cost extension until September 30, 2002 was submitted and approved. The statement of work for that extension included adjustment of ACE densities below wind speeds of 350 km/s, a study of shock normal orientations using travel time delays between the two spacecraft, comparison of density jumps at shocks, and a study of temperature anisotropies and double streaming to see if such features evolved between the spacecraft.

Our accomplishments over the final year of the project, which build upon the previously reported work, are outlined in Section 2.

2. ACCOMPLISHMENTS

We extended the original comparison of solar wind parameters from the 16-day study previously reported to cover the entire overlapping interval between the two missions. This larger dataset allowed us to perform a more statistically rigorous comparison of various solar wind parameters between the two spacecraft. Section 2.2 presents the results of that study. The two parameters with both the largest differences and largest variation between spacecraft are the thermal speed and the number density. We decided to explore these two more closely.

We feel in part that the differences in thermal speeds are due to the different analysis techniques employed by the two instruments, and due to the anisotropic nature of ion temperatures in the solar wind. This is discussed in more detail in Section 2.2, in which we present the results of a moment analysis of the Faraday Cup data mentioned in the previous reports.

The discrepancy between *ACE* and *Wind* densities was traced to a design flaw in the *ACE* instrument which caused their densities to be too low at wind speeds <350 km/s. That problem has been resolved by using *Wind* densities as a standard and adjusting the *ACE* densities accordingly. This recalibration was carried out by Dr. Ruth Skoug at LANL and has proved to be stable and reliable. Nevertheless there remains, on average, a difference in the densities measured by the two instruments. We continue to explore that problem, though on examination of particular events, the difference is small (see Section 2.2).

Meanwhile at MIT, we compared our densities with those obtained by the Thermal Noise Receiver (TNR) portion of the WAVES experiment on *Wind*. That experiment measures the plasma frequency, which only depends on the square root of the electron density. The densities were found to agree to better than 5% with a tail extending to higher TNR densities; periods during which the TNR densities were higher than those determined by the Faraday Cup experiment are thought to be times when heavy ion component of the wind contributes a significant number of electrons to the solar wind mix. A detailed study of such times is still underway, but overall the comparison with the independent measurements by TNR is excellent. Section 2.3 presents an overview of the results.

Finally, in Section 2.4, we present some new results in our study of the correlation of events propagating between the two spacecraft. In our previous reports we focused on correlation of general solar wind features but declared our interest in comparing interplanetary shocks seen by both spacecraft. Analyzed interplanetary shocks seen by both spacecraft and compared the predicted arrival time with the observed one.

2.1 COMPARISON OF ONE-HOUR AVERAGES

Our dataset for parameter comparison was extended to cover all solar wind observations over the entire period from January 1998 through August 2002. The average, median, and standard deviation of the proton bulk speed, velocity components, East-West (EW) and North-South (NS) flow angles, thermal speed (w), and proton number density (n) were calculated for each one-hour interval using *Wind* data and *ACE* data propagated to *Wind*. Instead of the original Key Parameter (KP) *Wind* data we used the results of a bi-Maxwellian analysis of the Faraday Cup hydrogen and helium data which allowed for temperature anisotropies, a factor which is taken into account in

the *ACE* analysis. This new *Wind* dataset has been submitted to the NSSDC and will be made public by them. As mentioned in the introduction, the *ACE* data have been recalibrated and their Level 2 files for the entire mission have been updated and were used in this study.

To limit the effects of spatial and temporal structure on the one-hour time scale the following restrictions were applied to the averages: At least 30 individual measurements must have been selected for calculating the averages; the spacecraft separation perpendicular to the solar wind flow must be less than 50 Earth radii; the fluctuation of the quantity under consideration (defined as the ratio of the standard deviation of the selected measurements to the median value) must be less than 5%. In total 22,000 one-hour intervals were selected for comparison.

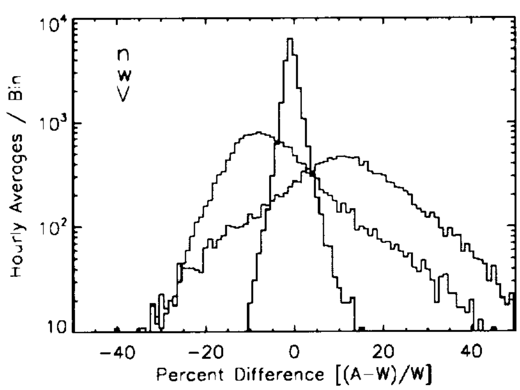

Figure 1: Histograms of the percentage differences between *Wind* and *ACE* bulk speeds, thermal speeds, and number densities.

In Figure 1 the histograms of the percent differences between *ACE* and *Wind* measurements are shown for the selected intervals for the bulk speed, thermal speed, and density. Table 1 is a summary of the mean values of the ratios and differences of each solar wind parameter.

Param.	Ratio (A/W)	Difference (A-W)
V	99.7%±2.6%	-1.3±10.7 *km/s*
V_x	99.7%±2.7%	1.3±10.8 *km/s*
V_y	N/A	-1.2±10 *km/s*
V_z	N/A	0.7±11 *km/s*
EW	N/A	-0.1±1.5 *degrees*
NS	N/A	-0.1±1.5 *degrees*
w	97.8%±14%	N/A
n	111.2±17%	N/A

Table 1: Overall comparison of one-hour averages of *Wind* and *ACE* observations.

The bulk speeds agree to within less than one percent, with *ACE* speeds on average 1.3 km/s or 0.3% less than the Wind speeds. On average the EW and NS flow angles agree to within 0.1 degrees. All the measured differences were within one standard deviation of being in agreement. The largest differences were in the thermal speeds and the number densities; and as described in Sections 2.2 and 2.3 we decided to explore these two quantities more closely.

2.2 DIFFERENCES IN THERMAL SPEEDS

On average the *Wind* and *ACE* thermal speeds differ by only 3%, but there is a large scatter in this difference, with an approximate width of 14%. Some portion of this disagreement may be caused by evolution of the solar wind as it propagates from *ACE* to *Wind* (e.g. turbulence, or adiabatic cooling), but we decided to determination of thermal speeds more closely, to identify possible instrumental sources of this scatter.

While the summary data of both instruments contains a single thermal speed, w, the solar wind is actually anisotropic, with one thermal speed $w_\parallel$ along the ambient magnetic field, and a second thermal speed $w_\perp$ perpendicular to the field. The *ACE* Level 2 dataset provides a "radial" thermal speed, which is the projection of the two thermal speeds along the Sun-Earth line. If the field at 1 AU were oriented in the typical Parker spiral, at an angle of approximately 45 degrees, than the radial thermal speed w_r would be given by,

$$w_r^{\,2} = \tfrac{1}{2}(w_\perp^{\,2} + w_\parallel^{\,2}) . \qquad (1)$$

On the other hand, the single thermal speed w_t reported by *Wind* investigation is calculated by taking the trace of the temperature tensor,

$$w_t^{\,2} = \tfrac{1}{3}(2w_\perp^{\,2} + w_\parallel^{\,2}) . \qquad (2)$$

The thermal speeds $w_\parallel$ and $w_\perp$ observed by *Wind* are seen to vary by factor of two from unity [Kasper, 2002]. Using equations (1) and (2) we would expect the ratio of the radial and trace thermal speeds to vary by ±6%.

In addition to the effect of anisotropy, there is the possibility that the analysis techniques used by the two instruments are responsible for the differences in thermal speeds. This possibility is mainly because the moment technique used by the *ACE* instrument is especially sensitive to any non-Maxwellian features in the ion distribution function, but in addition there are approximations which go into each method and they could produce different results. In our previous report we stated that we had begun a moment analysis of the Faraday Cup data.

We felt that applying both analysis methods to the observations of a single instrument would allow us to remove issues of solar wind structure and propagation effects. In all, two million *Wind* spectra were compared. Two dimensional histograms of the distribution of moment vs. non-linear thermal speeds are shown in Figure 2 for both parallel and perpendicular thermal speeds.

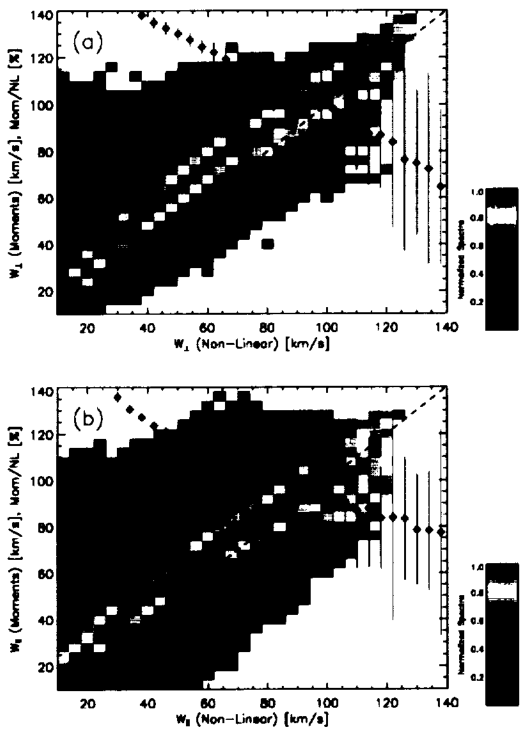

Figure 2: Comparison of moment and non-linear calculations of the perpendicular (a) and parallel (b) proton thermal speeds using *Wind* Faraday Cup observations. Colored bins indicate the normalized distribution of the observations; compare with the dashed line indicating equality. Diamonds indicate 100 x the average ratio as a function of speed.

We found that while the two methods generally agree, the moment thermal speeds are generally slightly larger (in agreement with our expectations). In addition, we identified a speed-dependent trend in the average ratio of the two thermal speeds. This trend was investigated further through the use of a series of Monte-Carlo simulations of solar wind spectra and Faraday Cup measurements. Figure 3 shows the results of the simulation. The diamonds are the observed variation of 100 x the ratio of the moment to non-linear thermal speeds. We ran three different simulations of solar wind ions and plotted the average and one sigma envelope for each run in a different color. The first simulation was based solely on the contribution of protons to the total signal produced in the Faraday Cup instruments. It reproduces the effect at large thermal speeds in which the moment thermal speeds are smaller than the non-linear thermal speeds. We believe that this is due to the fact that at large thermal speeds the instrument may not see the entire distribution, and as a result the second moment is underestimated.

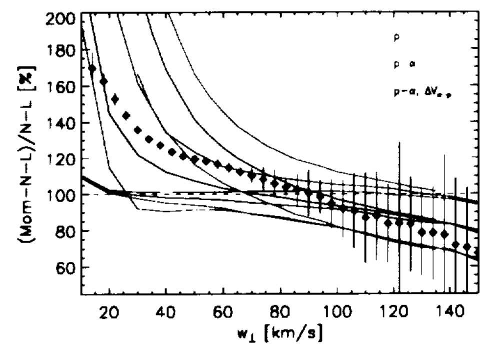

Figure 3: Comparison of the observed variation of the ratio of moment to non-linear calculations with Monte-Carlo simulation of ratio, as a function of bulk speed. For each of the simulations, the center line is the average value of 100 x the ratio of the moment over the non-linear thermal speeds, and the upper and lower lines indicate the one-sigma width of the distribution of simulated ratios.

The first simulation did not reproduce the correct behavior at small thermal speeds, so we added alpha particles to the simulation. The first results with alphas are shown in green. They did produce an upturn at low thermal speeds, which we interpret as a portion of the alphas being included in the calculation of the proton temperature. However, the effect was too large. We then produced the final run, in which a the alphas were allowed to stream along field lines, as is commonly observed at 1 AU. This resulted in the red curves, which were in good agreement with the observed ratios. We can conclude for the Faraday Cups that the two major sources of discrepancies are not seeing the entire distribution at large thermal speeds and contamination from alpha particles at small thermal speeds.

2.3 ACCURACY OF NUMBER DENSITIES

Following the same arguments in the previous section, we felt it was important to compare the Faraday Cup number density measurements with another instrument on Wind, to remove our study from the propagation and structure effects. We decided to compare the *Wind* densities with the total electron number density inferred by the observations

of the electron plasma frequency by the WAVES/TNR instrument on *Wind*.

A limited version of this study was conducted early in the *Wind* mission [Maksimovic, 1998], in which several days of FC proton number densities were compared with TNR inferred electron number densities. Several things have happened since: the TNR results were recalibrated and adjusted by several percent; the FC data was analyzed to produce helium densities; and a merged dataset was prepared containing more than two million solar wind observations, permitting a more statistically significant analysis.

It is especially important that we include the contribution of the helium to the total electron number density at a point in space. If the proton number density n_p, alpha number density n_α, and total electron number density n_e were all known, then we could define the fraction F_m of electrons which were due to minor ions such as oxygen and iron,

$$F_m \equiv 100\% \cdot \frac{n_e - n_p - 2n_\alpha}{n_e}. \qquad (3)$$

Theoretical calculations of F_m suggest that it should be somewhere between 2-4%, but that it may vary. We know, for example, that the abundance of helium in the solar wind varies as a function of speed and point in the solar cycle [Aellig, 2000]. The same effects might take place with minor ions, but they are less sensitive to the processes which effect the helium abundance.

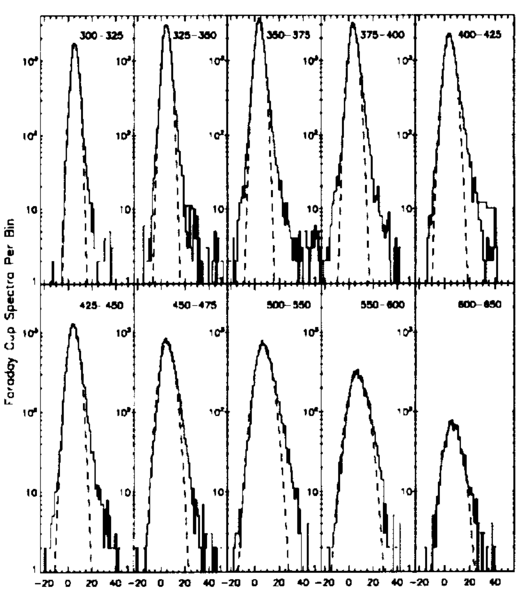

Figure 4: Histograms of the distribution of the measured values of F_m (3) as a function of bulk proton speed in ten windows.

We calculated a value of Fm for each Wind observation using the values of n_p and n_α from the Faraday Cups and n_e from the WAVES/TNR instrument.

Figure 4 is a plot of several histograms of the distribution of F_m as a function of solar wind speed in ten speed windows. These histograms only used data from 1998. The sections of the histograms highlighted in blue were then fit by Gaussian distributions. The red dashed curves are the best-fit Gaussians for each speed interval. Note that while each histogram is well-described by a Gaussian, the width and center is a function of speed.

This procedure was repeated for each year of the mission from 1995 through 2000. The results of our study are summarized in the two plots in Figure 5. The upper panel compares the width of the Gaussian distributions shown in Figure 4 with the average uncertainties in the measured densities. It is clear that the uncertainties in the Wind measurements are not sufficient to account for the natural width of the histograms of F_m. The lower plot shows F_m as a function of speed for six years of data. Note that all points are within 2% of the 2%-4% range in which we theoretically expect F_m. We conclude that the Wind Faraday Cup and TNR observations of densities are consistent to within 2%.

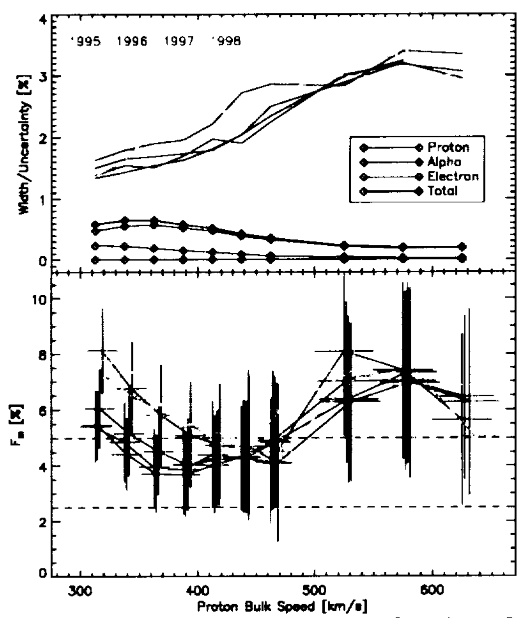

Figure 5: The variation of F_m as a function of solar wind speed and solar cycle. In the upper panel the width of the best-fit Gaussians are plotted as a function of speed, along with the average uncertainties of each of the measured densities. The lower panel is a plot of F_m as a function of speed for each year. The dashed lines indicate the expected range of F_m.

2.4 COMPARISON OF INTERPLANETARY SHOCK ARRIVAL TIMES

In the first two years of this project we focused on the correlation of general solar wind parameters as they propagated from *ACE* to *Wind*. We decided to look at the correlation of larger events, specifically interplanetary shocks, seen by both of the spacecraft. We had several motivations for this inquiry: interplanetary shocks are geoeffective events and their spatial correlation is of interest for space weather; there are certain physical properties of magnetohydrodynamic shocks which should not be violated (for example the ratio of downstream to upstream number density should not exceed a factor of four), so this is a chance to verify the physical validity of the measurements; observations of individual shocks by multiple spacecraft are an opportunity to test our understanding of the methods for characterizing shocks, and for probing the quality of the observations.

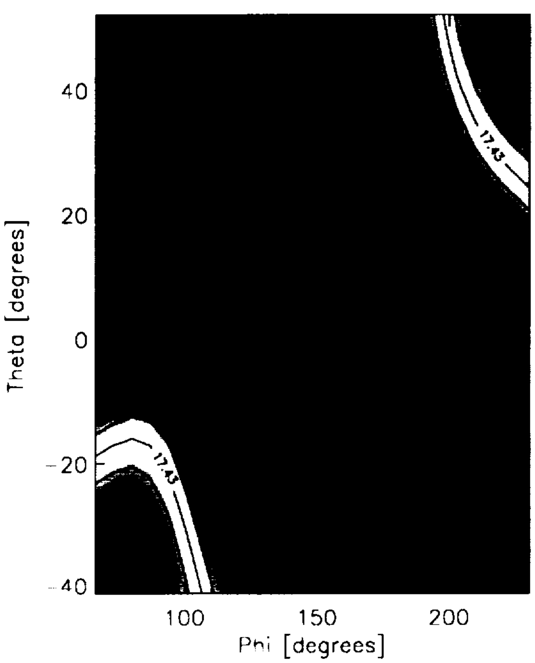

Figure 6: Comparison of shock normals determined by Wind using seven analysis techniques. The background color contour is the value of the χ^2 merit function as a function of possible shock orientation for the Rankine-Hugoniot analysis. Theta is the angle out of the ecliptic plane and phi is the azimuthal angle from $+X_{gse}$ to $+Y_{gse}$. The intersection of the dashed lines would be a radial shock. Each of the crosses indicates the normal as determined by each of the analysis methods.

Figure 6 displays the determinations of shock front normal from the seven most common shock analysis methods: magnetic coplanarity (MC), velocity coplanarity (VC), three mixed plasma-field methods (MX1,MX2,MX3), and the Rankine-Hugoniot relations (RH). The background color contour indicates the χ^2 per degree of freedom merit function from the RH method, with the minimum indicating the solution with the best fit to the data. Each of the crosses are the normal determined by other techniques, using the color code in Figure 7. Note in this case that all the methods agree to within several degrees, except for the magnetic coplanarity technique.

Altogether we have identified 120 fast forward interplanetary shocks which were observed by both *Wind* and *ACE*. We tested the effectiveness of each of the shock analysis methods, and the validity of the plasma measurements, by comparing the time delay for the shock to travel from one spacecraft to the other with the predicted time lag based upon the experimentally measured shock speed and direction. Shock arrival times were identified using high-resolution magnetic field data from *Wind* (3-second) and *ACE* (16-second) instruments. The typical uncertainty in the measured time lag was approximately 30 seconds.

Overall, the RH method produced the minimum difference between the predicted and observed time delays. This result was presented at the SHINE 2002 meeting. In addition, the time delays were studied as a function of the separation of the spacecraft perpendicular to the shock normal. As shown in Figure 7, we find that in general the methods become less accurate with increasing spacecraft separation, with the exception of the RH analysis, which maintains the same typical difference out to spacecraft separations of 340 Earth radii.

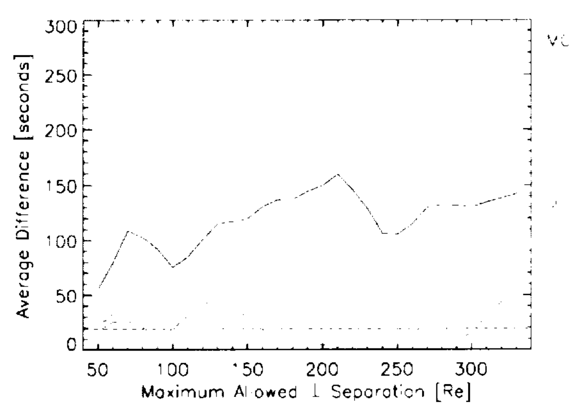

Figure 7: Average difference between predicted and observed shock arrival times as a function of spacecraft separation.

3. PRESENTATIONS

Steinberg, J. T., J. T. Gosling, D. J. McComas, R. M. Skoug, R. L. Tokar, A. J. Lazarus, and K. I. Paularena, "ACE and Wind: Comparison of Solar Wind Proton and Alpha Particle Measurements", AGU Spring 2002.

Clack D., Lazarus A., Kasper J., Kaiser M. "Wind SWE observations of proton double streaming and correlations with wave activity", AGU Fall Meeting, 2001.

Jurac S., Kasper J. C., Richardson J. D., Lazarus A. J., "The geoeffective scale sizes of solar wind events", AGU Fall Meeting, 2001.

Tanabe J. T., Kasper J. C., Lazarus A. J., "Proton and Alpha Particle Temperature Anisotropies in the Solar Wind with the WIND/SWE Faraday Cup", AGU Spring Meeting, 2001.

Jurac S., Kasper J. C., Richardson J. D., Lazarus A. J., "On the Geoeffectiveness of Interplanetary Shocks", AGU Spring Meeting, 2001.

Kasper, J. C., "Comparison of Interplanetary Shock Analysis Techniques", SHINE Workshop, 2002.

4. REFERENCES

Kasper, J. C., A. J. Lazarus, and S. P. Gary, "Wind/SWE observations of firehose constraint on solar wind proton temperature anisotropy", *Geophys. Res. Lett.*, **29**, 1839, 2002.

Kasper, J. C., "Solar Wind Plasma: Kinetic Properties and Micro-Instabilities", Thesis for Doctorate in Physics, Massachusetts Institute of Technology, 2002.

Maksimovic, M., J.-L. Bougeret, C. Perche, J.T. Steinberg, A.J. Lazarus, A.F. Viñas, and R.J. Fitzenreiter, "Solar wind density intercomparisons on the WIND spacecraft using WAVES and SWE experiments", *Geophys. Res. Lett.*, **25**, 1261-1264, 1998.

APPENDIX 1

Progress Report for Wind-ACE G.I. Grant
NASA NAG5-7794
MIT 6792900
August 6, 1999

INTRODUCTION

Our study has two main goals:

1) The inter-calibration of solar wind parameters measured on the two spacecraft

2) Cross-correlation of the measured solar wind parameters for the purpose of determining the spatial scale of solar wind features and for input to the Space Weather Program.

During 1998 ACE was in a halo orbit about L1 with a halo radius of about 35 Re. Early in 1998, WIND was in a large L1 loop, which brought it close to ACE. Later in 1998, WIND was in phasing loops with apogees between 100 and 150 Re. These orbits allowed correlation studies as a function of separation distance.

PROGRESS TO DATE

To fulfill the first objective, we compared solar wind parameters during a 16-day period when the two spacecraft were within 25 Re of one another (1998, days 83.5 to 99.5). Our findings were reported at the June, 1999 AGU meeting (EOS, S264, 1999) and are described below. Both data sets are public and widely distributed: the Wind Key Parameters and the ACE Level 2 data.

Figure 1 shows hourly-averaged parameters for Wind and ACE for the 16-day interval. Overall, the large-scale features track well as viewed from both spacecraft: significant rises or falls in all parameters are seen from both spacecraft. In detail, the speeds agree most closely, while the ACE density is at times systematically higher than the WIND density. The ACE SWEPAM is known to have an energy-dependent response, which results in a lowered counting rate and hence greater statistical uncertainty in determining solar wind fluxes when speeds are below 350 km/s. Therefore we expect ACE and WIND disagreements to be greater at the lowest speeds. This low speed effect is apparent in Figure 1, although it does not account for all Wind/ACE differences. Much of the temperature difference can be accounted for by the different analysis techniques applied to the two data sets; Wind analysis uses a fit to a convected Maxwellian; ACE uses a moment calculation. The WIND fits are expected to be produce lower temperatures values than the ACE moments since the presence of a non-Maxwellian high-energy tail is quite common.

Figures 2, 3, and 4 show scatter plots and histograms comparing parameters over the full time period when the spacecraft were within 25 Re. Figure 2 shows the expected good correlation in derived speeds. On average, Wind speeds appear to be about 1% higher that those from ACE.

Figure 3 compares the density estimates. Although the correlations are reasonably good, the histogram shows a wide distribution of differences. This spread needs further explanation, and we plan to try to relate it to specific temporal events.

Figure 4 compares the derived temperatures. We believe some of the differences are due to

using moments rather than Maxwellian fits for the ACE data. On the other hand, there are clear examples when the velocity distributions are not Maxwellian (for example they might have a power- law high-energy tail), and we need to try moment analysis of the Wind data before we can determine the reasons for the disagreements.

Figures 5a and 5b show the parameters determined by Wind (black) and ACE (red) during day 312 when they were separated by about 100 Re. During that period, the speed of the wind was higher than 350 km/s; at those speeds the ACE parameters are in a more reliable range. The ACE data have been "time lagged" to the Wind data by maximizing the correlation of proton speeds; the time delay is approximately 30 minutes. The differences in the parameters are striking: although the densities from ACE are generally higher, there is clear evidence near 312.89 for a structure that is spatially smaller at ACE. After 312.92, the densities track very well, as they do near 312.65. Those plots also show that the alpha particle structures correlate differently from the proton structures during the same time interval. Clearly, those differences warrant further work.

Resolution of the differences in parameters from the two spacecraft thus lies in understanding the spatial structure of the wind itself as well as in further exploration of the analytical techniques. Our conclusion is that comparisons over distances ranging from less than 25 Re to approximately the distance from L1 to Earth are not simple, and further work needs to be done.

The second objective of our joint study is to look at correlations between measurements taken from spacecraft at varying distances from one another. Previous work has been done on this topic using IMP 8, Wind, ISEE-3 and Interball by Paularena, Richardson, Zastenker, and Lazarus.

The same technique that had been used in the earlier studies was used here: measurements from a six-hour time interval were shifted in time to correspond to the XSE distance between the spacecraft using the average measured speed; the data were then interpolated to the same time scale; and an additional time shift was made to maximize the cross-correlation between the parameters.

The results from the time period between February 5 through end of 1998 are shown in Figure 6 for the entire period (times when Wind was not in the solar wind were deleted). The additional lags to achieve the best correlations are shown in the left set of panels, and the correlations as a function of the spacecraft separation in the YGSE coordinate are shown in the right set of panels. The time lag series of panels is consistent with structure alignment roughly along the Parker spirals. The variation of correlation with YGSE separation is not yet understood.

Figure 7 shows the correlations as a function of XGSE separation. There is no clear trend, though ISEE-3/IMP 8 studies showed a decreasing correlation with greater XGSE separation. (The error bars show the standard deviations of the distributions whose means are plotted as a histogram. The uncertainties of the means are much smaller than the error bars.)

Figure 8 shows the correlations as a function of velocity and density. Note the relatively poorer correlation of densities at speeds below about 350 km/s due to lower count rates and hence greater uncertainty in the ACE data, as mentioned earlier.

Note that the average correlations are of the order of 0.7 as in previous studies. The correlations for large events may well be better, but the differences seen in Figures 5a and 5b suggest that the intrinsic spatial scales of the solar wind are small enough to be important in

making predictions based on observations at L1.

FUTURE WORK

It should be clear that we have made progress but that there is much to be done. We already have good data sets that raise interesting questions.

1) The task of relating the two sets of observations taken when the spacecraft are relatively close together is not finished: additional corrections need to be made to the acceptance function of the ACE instrument, the histograms of the parameter differences show that we must also cross compare analysis techniques, and there are intrinsic differences due to the solar wind spatial scales that need to be teased out. The WAVES experiment on Wind gives a near absolute measure of the density, but the details of the distribution functions need to be examined.

2) We want to relate the correlation variations to the nature of the flows being observed: CMEs, high-speed steams, and high or low density regions. The Wind/IMP comparisons suggest that "fronts" of different plasma conditions are aligned half way between the Parker spiral and the direction normal to the Sun-Earth line. Wind, IMP, and ACE observations of the same fronts can help pin down their orientations under different conditions,

3) A preliminary look at the alpha particle data suggests correlations that differ from those of the protons during the same time interval.

4) We want to include the Wind/SOHO correlations for the same time intervals.

5) We want to study particular intervals such as the low density region seen at ACE and Wind on May 11-12, 1999:

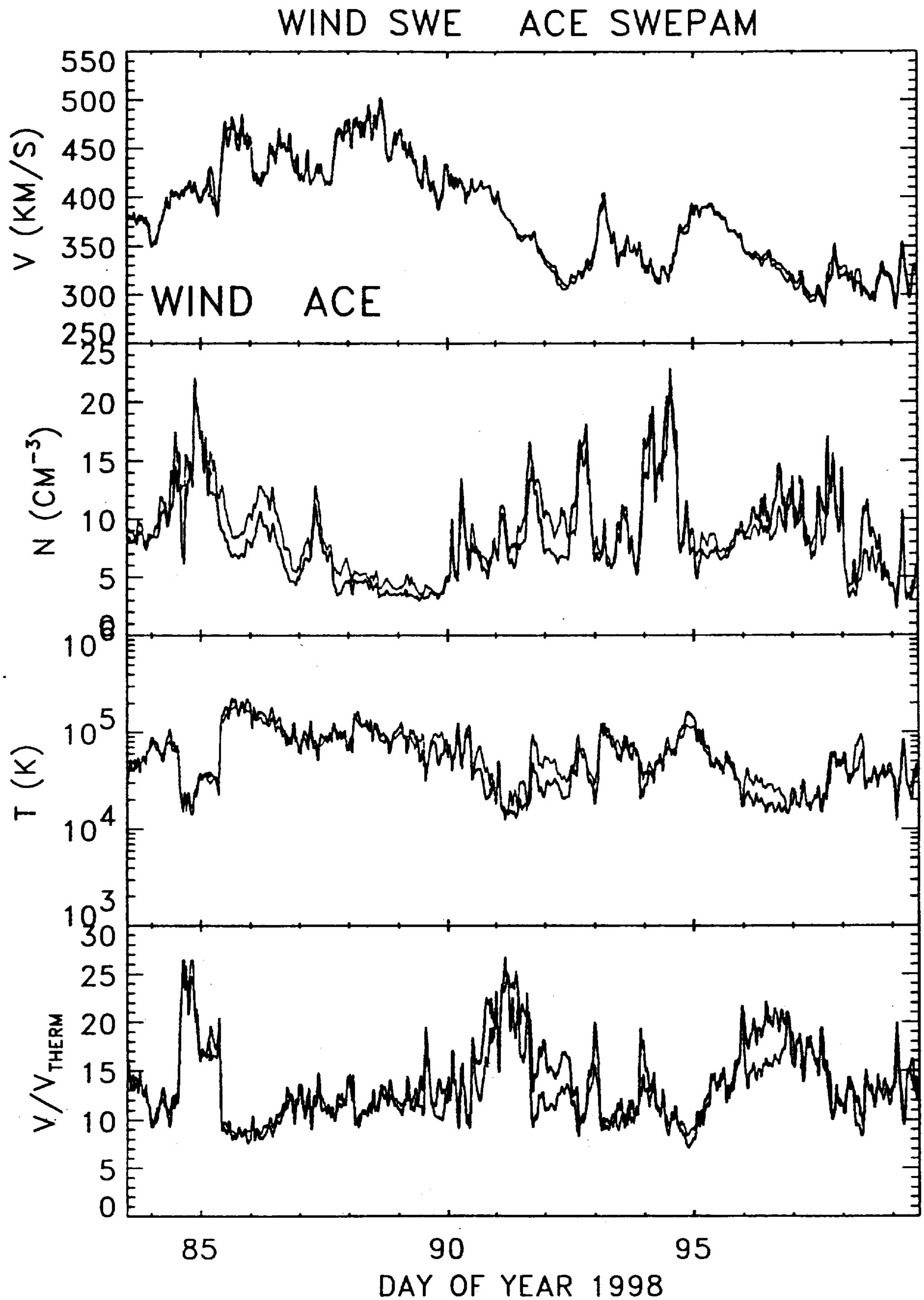
WIND SWE ACE SWEPAM
WIND ACE
V (KM/S)
550
500
450
400
350
300
250
N (CM^{-3})
25
20
15
10
5
0
T (K)
10^6
10^5
10^4
10^3
V/V_{THERM}
30
25
20
15
10
5
0
85
90
95
DAY OF YEAR 1998

Figure 1

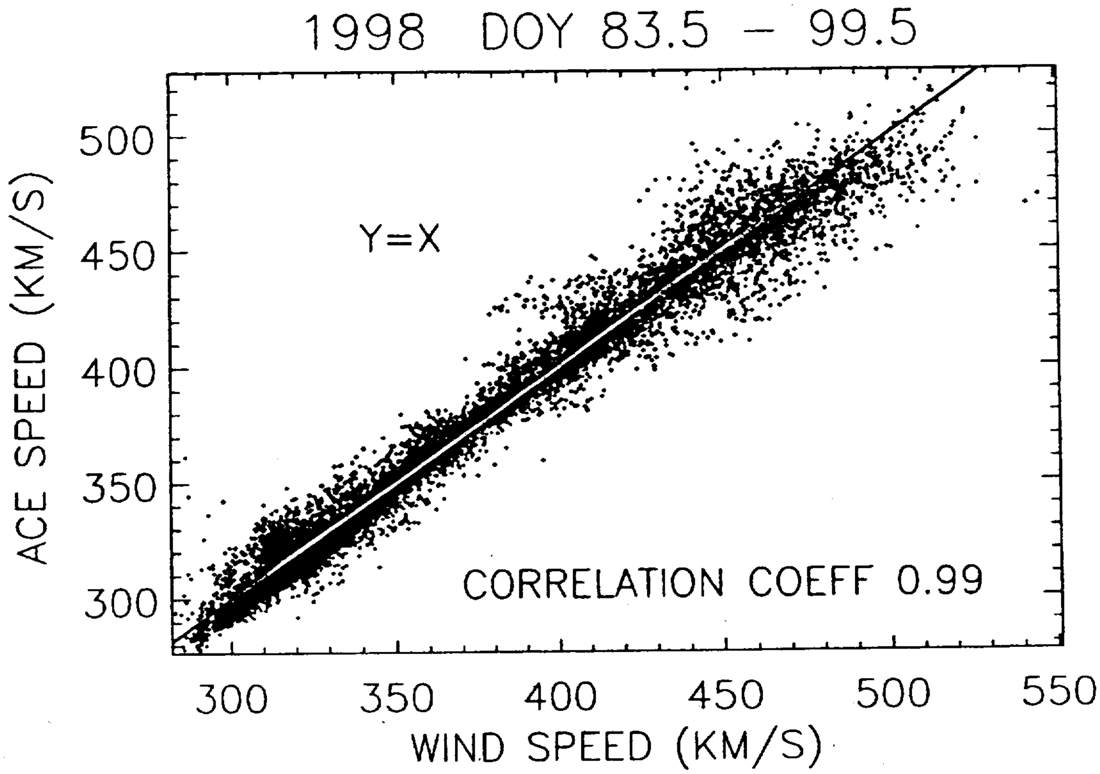
1998 DOY 83.5 – 99.5
Y=X
CORRELATION COEFF 0.99
ACE SPEED (KM/S)
WIND SPEED (KM/S)
300
350
400
450
500
550

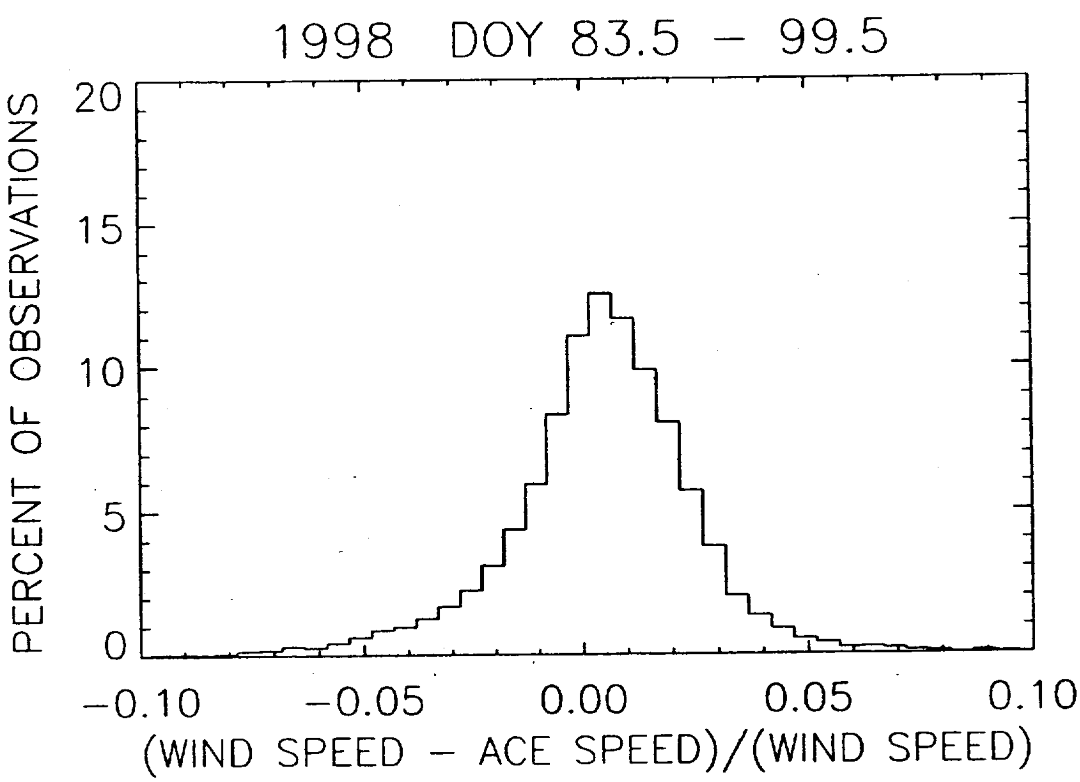
1998 DOY 83.5 – 99.5
PERCENT OF OBSERVATIONS
(WIND SPEED – ACE SPEED)/(WIND SPEED)
0
5
10
15
20
−0.10
−0.05
0.00
0.05
0.10

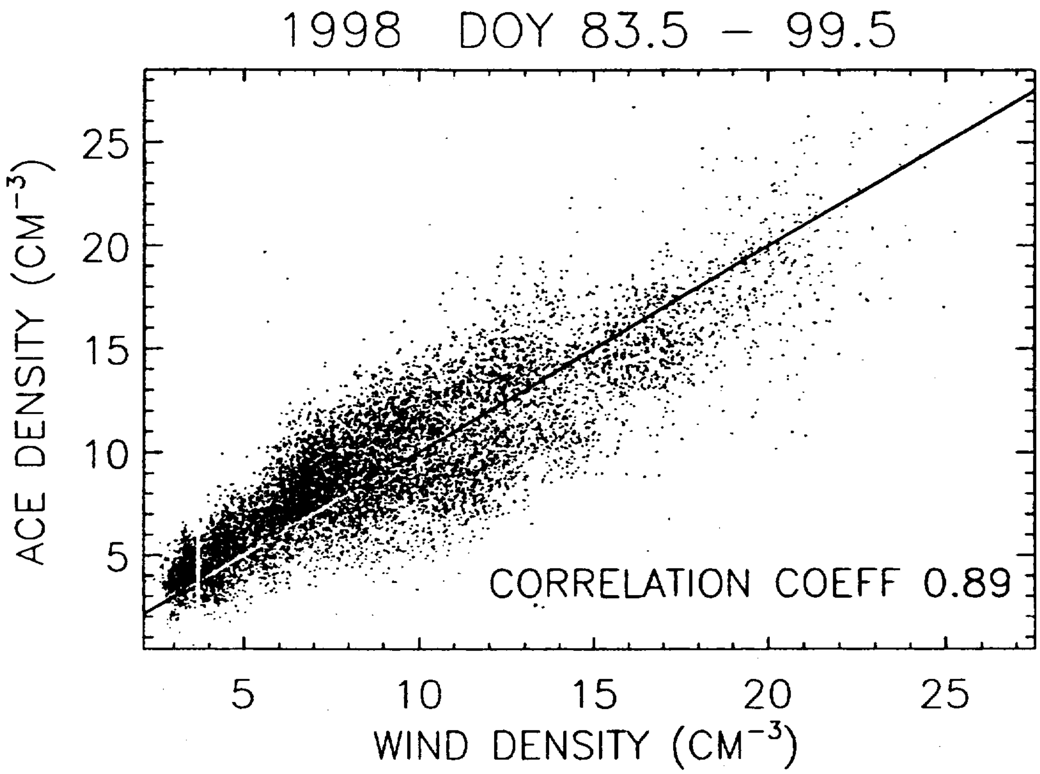
1998 DOY 83.5 – 99.5
ACE DENSITY (CM^{-3})
WIND DENSITY (CM^{-3})
CORRELATION COEFF 0.89
5
10
15
20
25

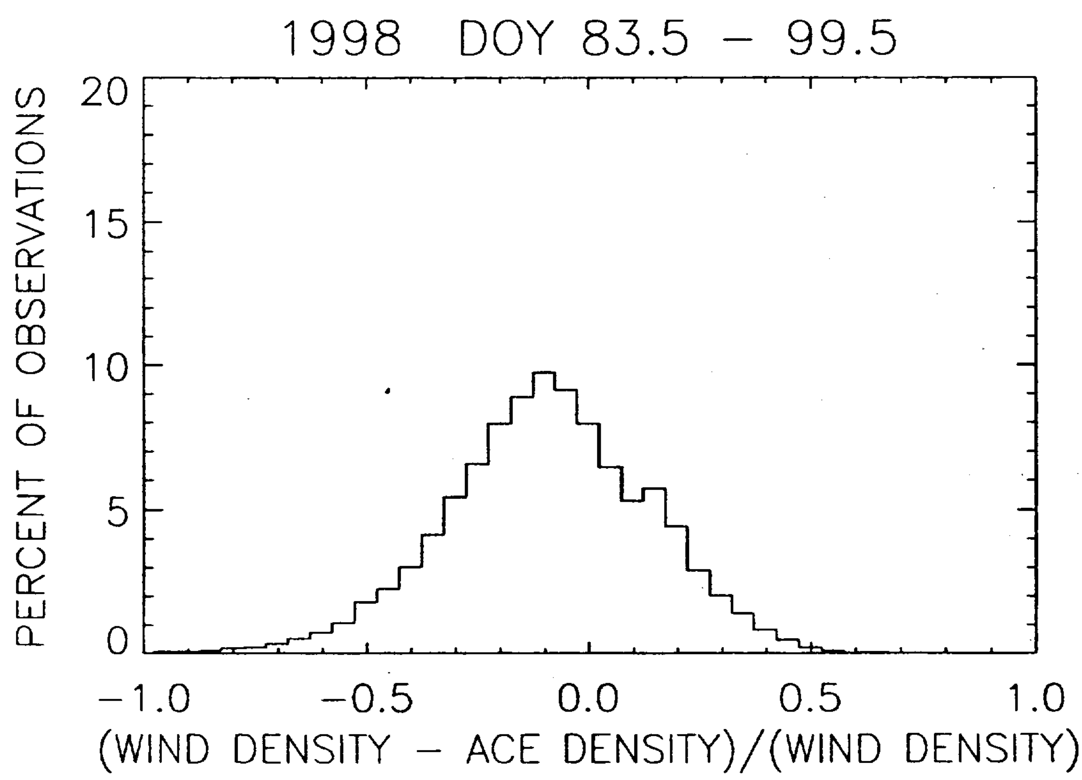
1998 DOY 83.5 – 99.5
PERCENT OF OBSERVATIONS
(WIND DENSITY – ACE DENSITY)/(WIND DENSITY)
0
5
10
15
20
−1.0
−0.5
0.0
0.5
1.0

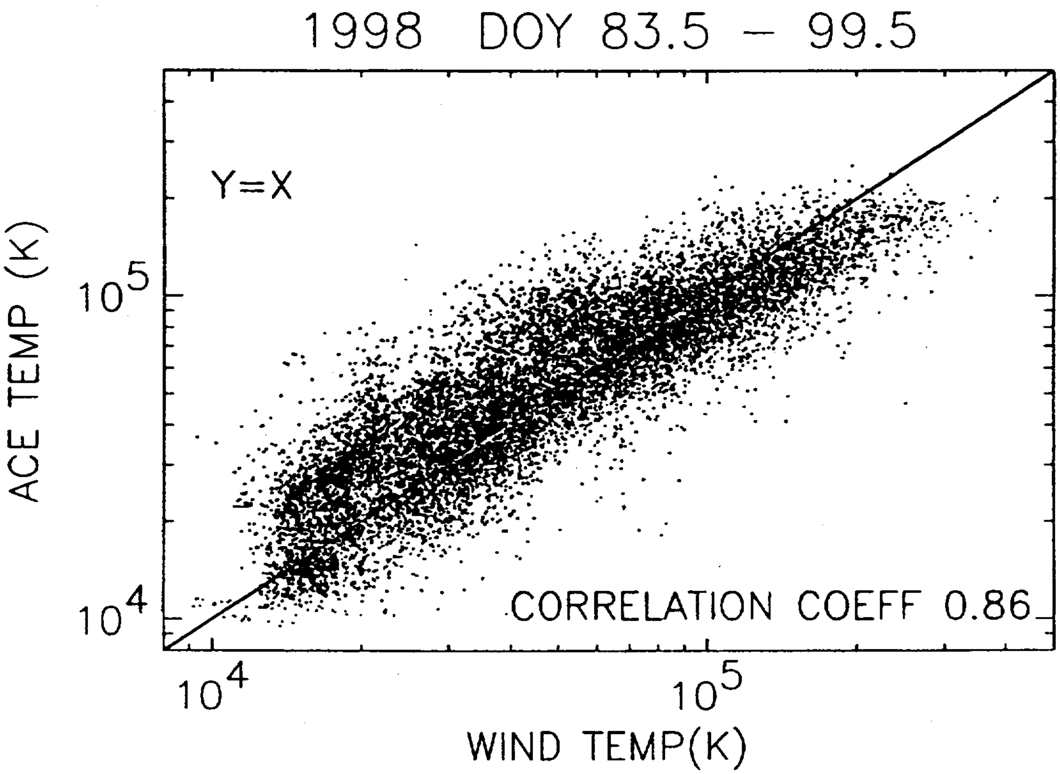
1998 DOY 83.5 − 99.5
Y=X
CORRELATION COEFF 0.86
ACE TEMP (K)
WIND TEMP(K)
10^5
10^4
10^4
10^5

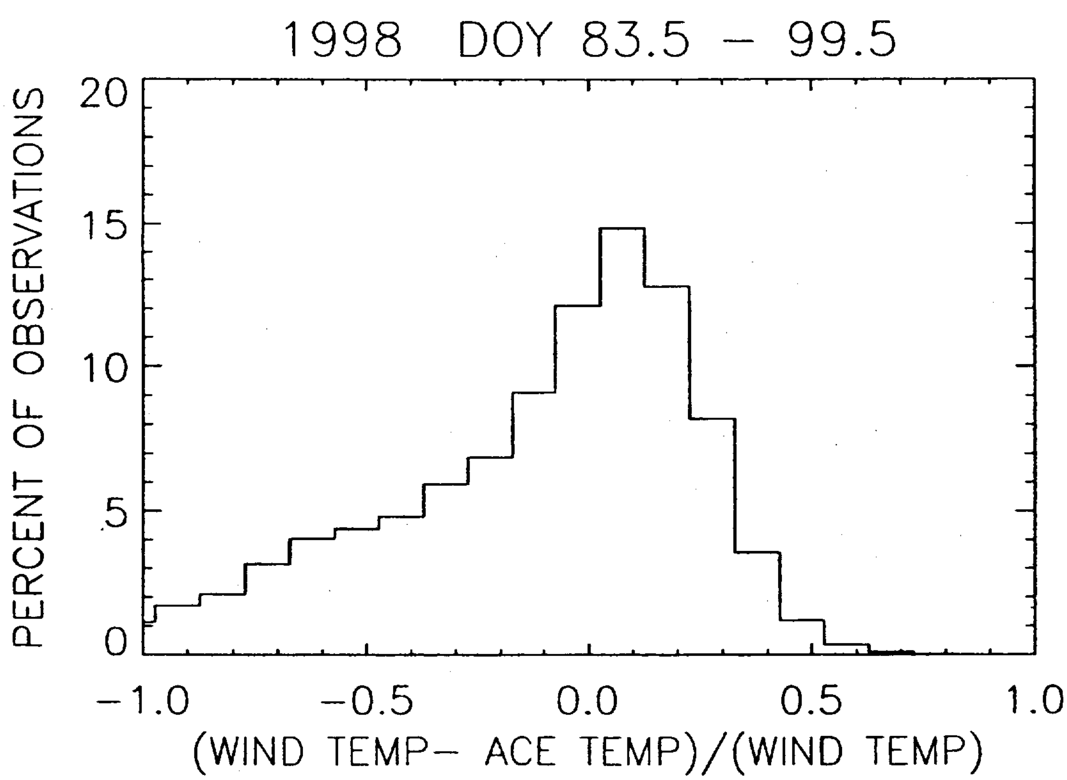
1998 DOY 83.5 − 99.5
PERCENT OF OBSERVATIONS
(WIND TEMP− ACE TEMP)/(WIND TEMP)
20
15
10
5
0
−1.0
−0.5
0.0
0.5
1.0

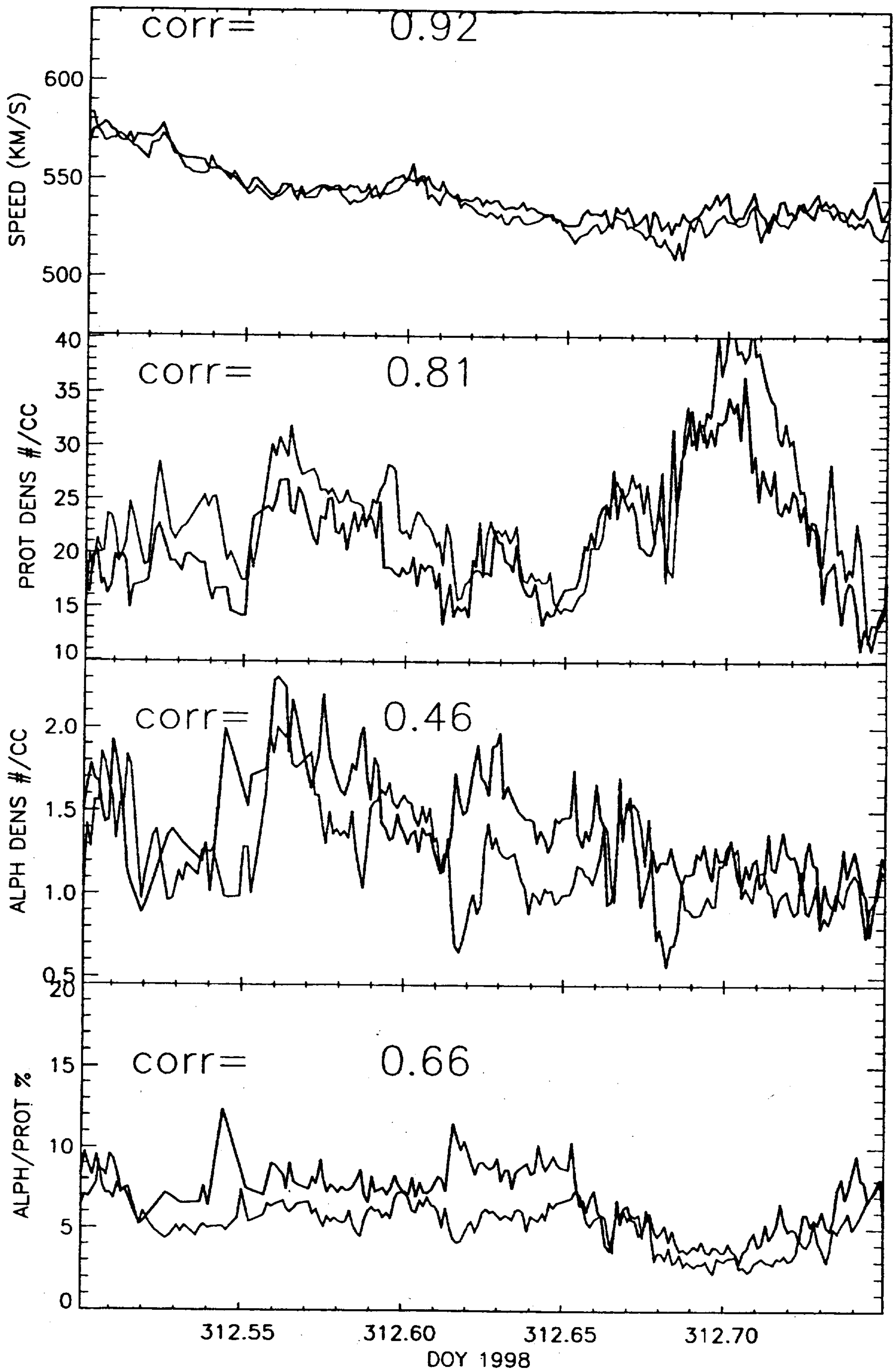

corr= 0.92
SPEED (KM/S)
600
550
500
corr= 0.81
PROT DENS #/CC
40
35
30
25
20
15
10
corr= 0.46
ALPH DENS #/CC
2.0
1.5
1.0
0.5
corr= 0.66
ALPH/PROT %
20
15
10
5
0
312.55
312.60
312.65
312.70
DOY 1998

5a

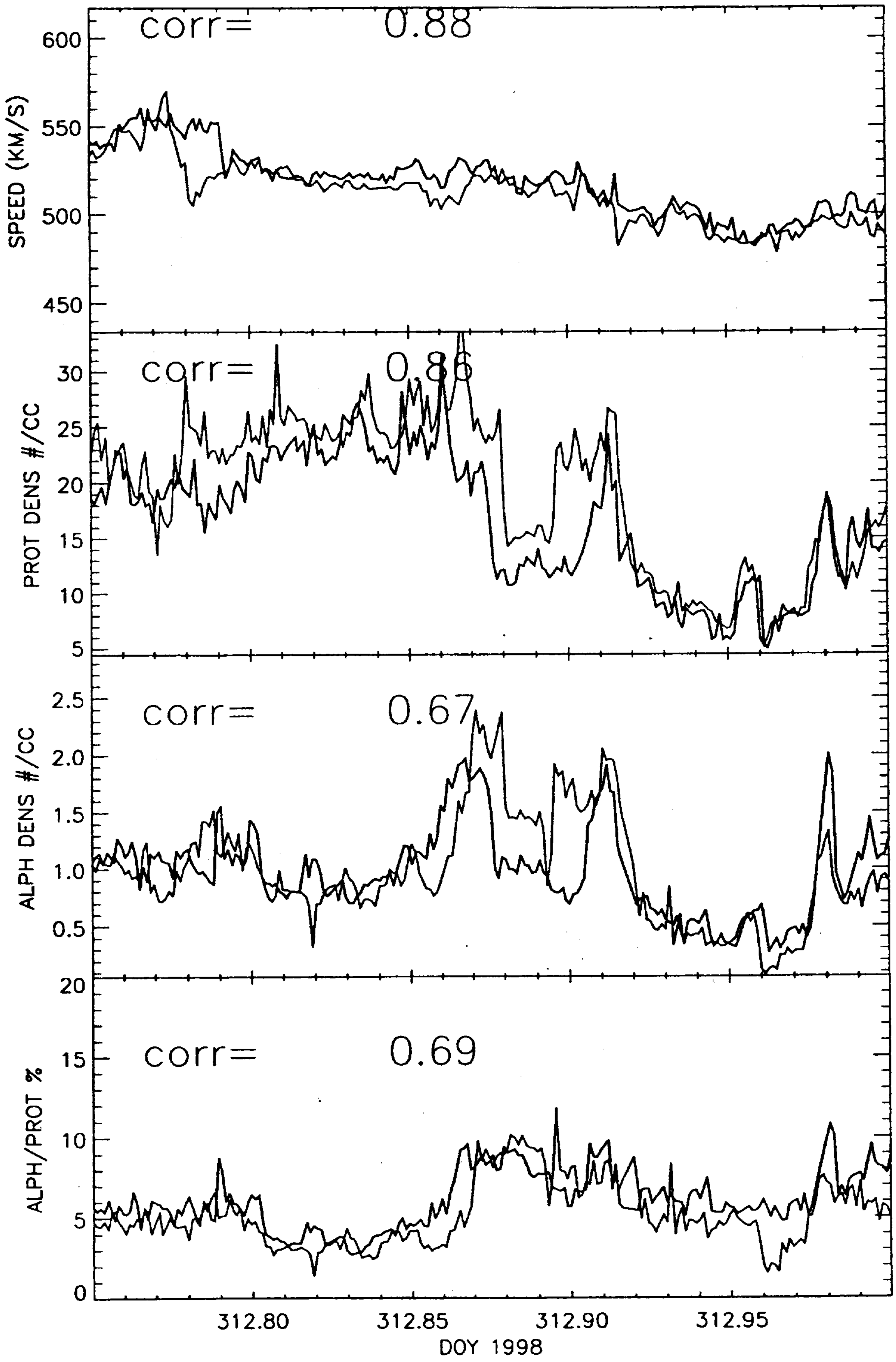

corr= 0.88
SPEED (KM/S)
600
550
500
450
corr= 0.86
PROT DENS #/CC
30
25
20
15
10
5
corr= 0.67
ALPH DENS #/CC
2.5
2.0
1.5
1.0
0.5
corr= 0.69
ALPH/PROT %
20
15
10
5
0
312.80
312.85
312.90
312.95
DOY 1998

5b

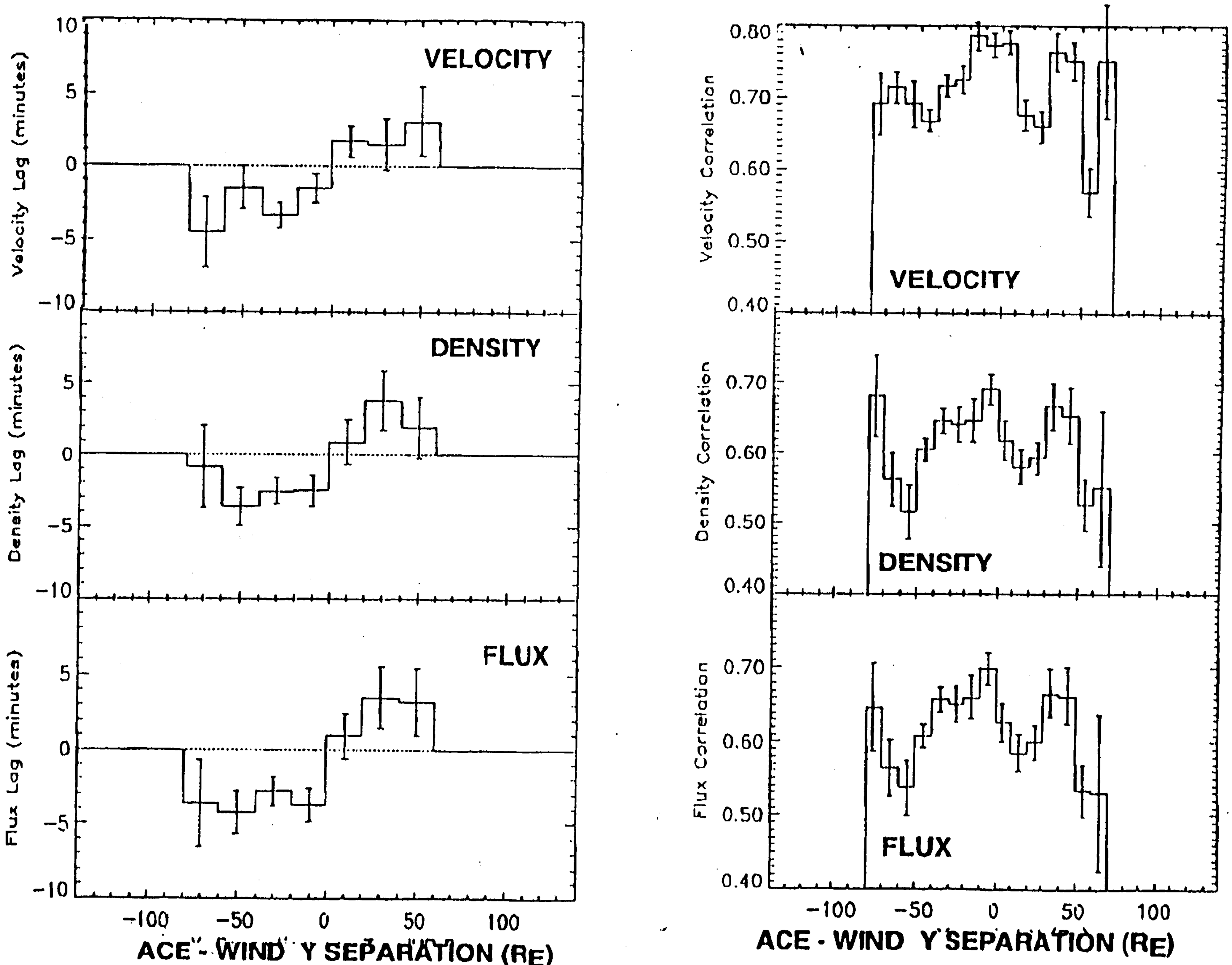
VELOCITY
DENSITY
FLUX
Velocity Lag (minutes)
Density Lag (minutes)
Flux Lag (minutes)
ACE - WIND Y SEPARATION (RE)
Velocity Correlation
Density Correlation
Flux Correlation

Figure 6

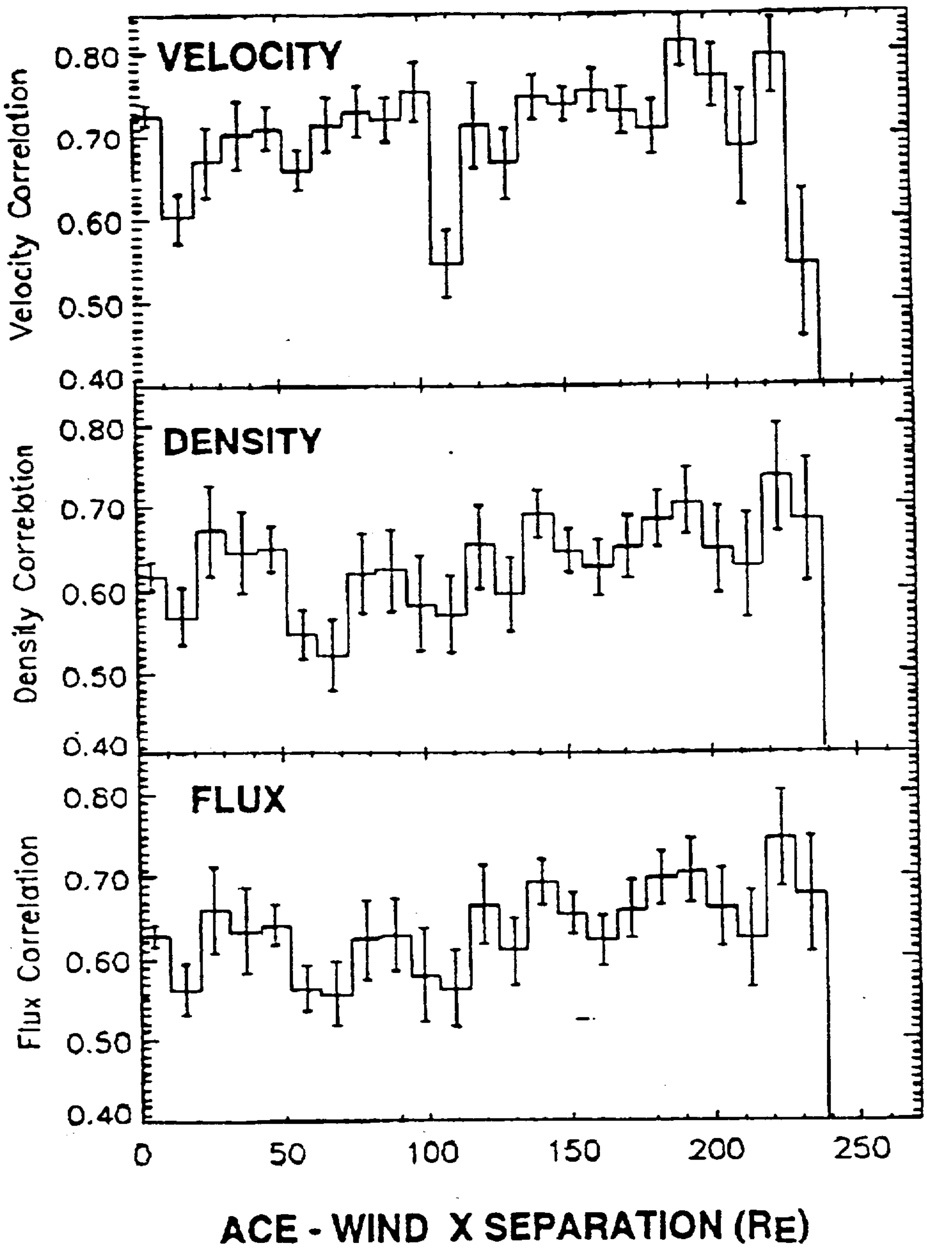

VELOCITY
Velocity Correlation
0.80
0.70
0.60
0.50
0.40
DENSITY
Density Correlation
0.80
0.70
0.60
0.50
0.40
FLUX
Flux Correlation
0.80
0.70
0.60
0.50
0.40
0
50
100
150
200
250
ACE - WIND X SEPARATION (RE)

Figure 7

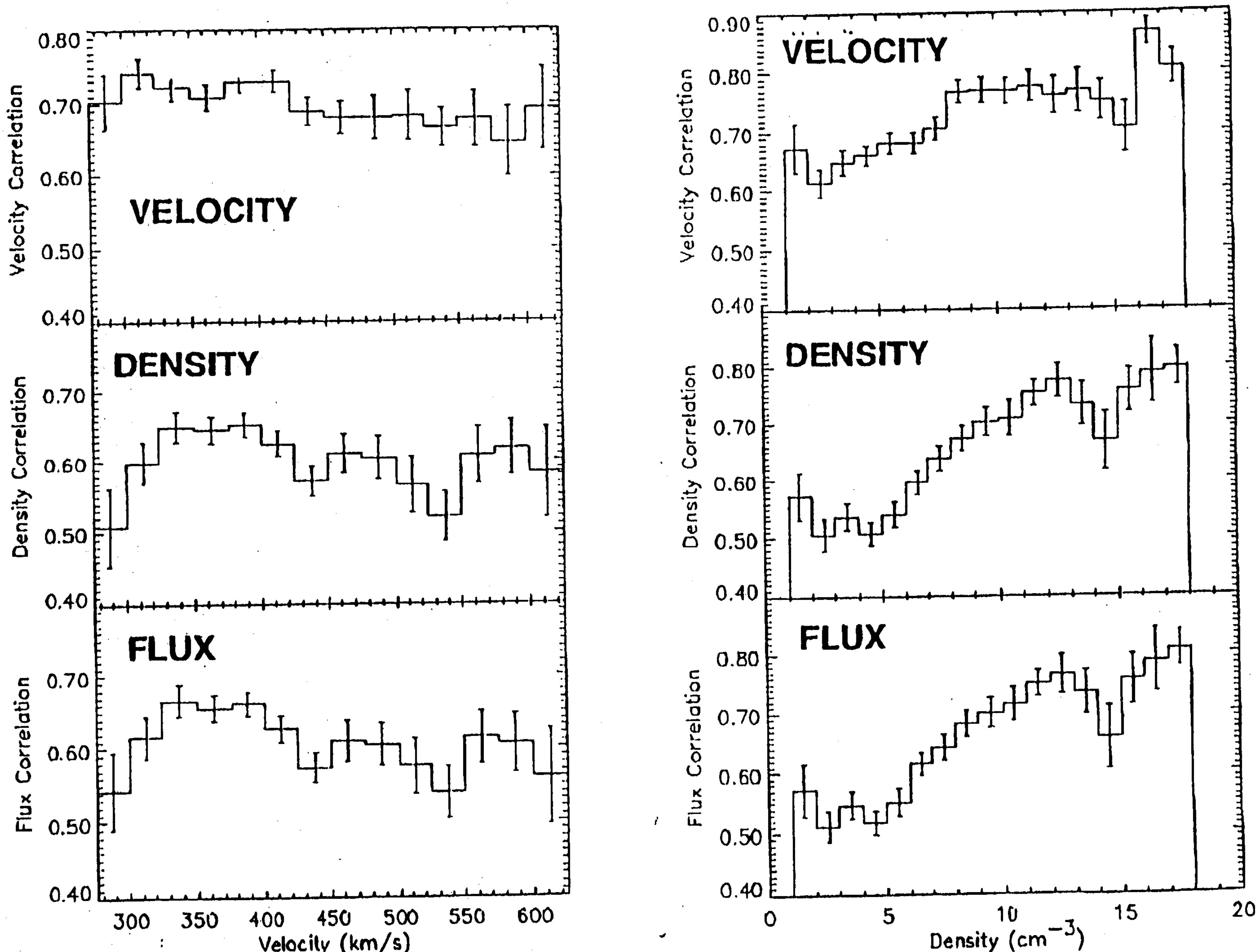
VELOCITY
DENSITY
FLUX
Velocity Correlation
Density Correlation
Flux Correlation
0.80
0.70
0.60
0.50
0.40
300 350 400 450 500 550 600
Velocity (km/s)
0.90
0 5 10 15 20
Density (cm^{-3})

Figure 8

Progress Report for Wind-ACE G.I. Grant
NASA NAG5-7794
MIT 6792900
October 26, 2000

INTRODUCTION

Our study has two basic goals:

1) The inter-calibration of solar wind parameters measured on the two spacecraft

2) Cross-correlation of the measured solar wind parameters for the purpose of determining the spatial scale of solar wind features and for input to the Space Weather Program.

During 1998 ACE was in a halo orbit about L1 with a halo radius of about 35 Re. Early in 1998, WIND was in a large L1 loop, which brought it close to ACE. Later in 1998, WIND was in phasing loops with apogees between 100 and 150 Re. These orbits allowed correlation studies as a function of separation distance. Now Wind is in an orbit which takes it to several hundred Re in the YGSE direction while remaining close to XGSE = 0. Thus we can use ACE/Wind comparisons to explore the spatial extent of solar wind events.

PROGRESS TO DATE

We took steps to carry out the work proposed in last year's status report.

We realized that some of the discrepancies between Wind and ACE observations could be attributable to the different analysis techniques employed: on Wind we typically have used a non-linear, least-squares method which attempts to fit the observed energy/charge spectra to spectra that would be expected from convecting, isotropic Maxwellian distributions; the ACE analysis technique uses moments of the observed velocity distributions to determine the parameters characterizing the solar wind. We have now redone the Wind analysis using both techniques. To date we have compared only selected portions of the data bases. It is clear that moment techniques are more sensitive to fluxes beyond the peak of the proton distribution and higher temperatures can result; on the other hand, fitting techniques could miss the contribution of a non-Maxwellian tail. We have just started this comparison, but by doing so we can recognize features which are really different at the two spacecraft positions and thus gain the ability to study evolution of features with distance.

We have just carried out the initial analysis data from the "Bastille Day" interval around July 14, 2000. That period is especially interesting to recover from both Wind and ACE because of several shocks related to a CME. (The CME was accompanied by large fluxes of energetic particles which dramatically increased the background noise on Wind's Sun sensor and thus confused the sun-pulse generator to the point that a default spin period was generated. That default period caused the data taking sequence of the Faraday Cup to make measurements at unusual angles and also caused the data buffers in the DPU to reject portions of the data. As a result, disentangling the true look angles and compensating for missing data has been a laborious process.) There were three shocks during the July 13-15 period. Wind is at XGSE near 0 but at YGSE = -60 Re, while ACE is near L1 but at +20 Re YGSE.

The three shocks have different character. The second shock shows a classic driver gas as well as the shocked plasma and the shock itself. The final shock is driven by plasma at speeds which Wind shows to be at about 1200 km/s but the ACE data suggests that the speeds are limited to about 900 km/s. Whether this speed difference is due to different spatial locations or is an artifact of the analysis is a topic for immediate attention, though it certainly underlines the value of having multiple observations of important events.

PROPOSED JOINT STUDIES FOR THE COMING YEAR

1. We plan to finish the comparison of solar wind parameters in order to both cross-calibrate the instruments but also to identify features which indicate spatial or evolutionary aspects of the wind. The specific study indicated next is only one of the possibilities. The data sets for such a parameter comparison now exist, and the comparison will be very helpful to both groups.

2. John Steinberg at LANL has examined alpha and proton behavior during periods with clear Alfvenic waves. The alphas have a larger velocity component along the magnetic field and tend to "surf" on the waves, while proton velocities are clearly correlated with variations in the magnetic field. He has identified at least one period when the Wind data (taken downstream from ACE) show both alphas and protons taking part in the waves. His hypothesis is that we are observing the evolution of the waves and their effects as the wind travels between the spacecraft. Peter Gary's analysis at LANL suggests that the spacing between the two s/c may be sufficient to see the growth of the instability that could cause the alphas to begin to participate in the waves.

3. Finally, the recent ISTP meeting at UCLA brought out the usefulness of categorizing pressure pulses in the wind, which are mainly due to density variations. Comparing observations of such pulses (their rise time, duration, and fall times) can be very useful for understanding the reactions of the magnetosphere to the resulting pressure changes.

FINANCIAL

We hereby request that NASA release the funding for this work at the heretofore agreed-upon amount of $69,243.

ALAN LAZARUS